Polymer Journal
https://doi.org/10.1038/s41428-021-00518-7

ORIGINAL ARTICLE

Thermoelectric properties of polypropylene carbon nanofiber melt-mixed composites: exploring the role of polymer on their Seebeck coefficient

Antonio José Paleo[1] · Beate Krause[2] · Maria Fátima Cerqueira[3,4] · Manuel Melle-Franco[5] · Petra Pötschke[2] · Ana María Rocha[1]

Received: 19 February 2021 / Revised: 21 April 2021 / Accepted: 19 May 2021

Abstract

The effect of polypropylene (PP) on the Seebeck coefficient (S) of carbon nanofibers (CNFs) in melt-extruded PP composites filled with up to 5 wt. % of CNFs was analyzed in this study. The as-received CNFs present an electrical conductivity of ~320 S m^{-1} and an interesting phenomenon of showing negative S-values of $-5.5\,\mu VK^{-1}$, with $10^{-2}\,\mu W/mK^2$ as the power factor (PF). In contrast, the PP/CNF composites with 5 wt. % of CNFs showed lower conductivities of ~50 S m^{-1}, less negative S-values of $-3.8\,\mu VK^{-1}$, and a PF of $7 \times 10^{-4}\,\mu W/mK^2$. In particular, the change in the Seebeck coefficient of the PP/CNF composites is explained by a slight electron donation from the outer layers of the CNFs to the PP molecules, which could reduce the S-values of the as-received CNFs. Our study indicates that even insulating polymers such as PP may have a quantifiable effect on the intrinsic Seebeck coefficient of carbon-based nanostructures, and this fact should also be taken into consideration to tailor conductive polymer composites with the desired thermoelectric (TE) properties.

Introduction

The seeking of high-performance thermoelectric (TE) materials able to transform a temperature gradient into an electrical voltage according to the Seebeck or TE effect constitutes currently a promising avenue towards a better use of available energy resources [1]. In practical terms, the performance of TE materials is generally assessed by a dimensionless figure of merit (zT), defined as $zT = \frac{S^2\sigma}{k}T$, where σ is the electrical conductivity, k is the thermal conductivity, T is the absolute temperature, and S is the Seebeck coefficient, calculated by $S = \frac{\Delta V}{\Delta T}$, where ΔV is the measured voltage at a temperature difference ΔT [2]. S can be positive or negative depending on the type of the majority charge carrier. Hence, in p-type TE materials (positive S), there is dominant hole conduction, whereas in n-type TE materials (negative S), the majority of the charge carriers are electrons [3]. In addition, the term $S^2\sigma$, known as the power factor (PF), can also be adopted to analyze the TE effectiveness. Accordingly, materials with large S, high σ, and low k values are necessary for the achievement of high TE properties. In this respect, inorganic materials such as Bi_2Te_3, PbTe, Sb_2Te_3, and their alloys have been intensively studied [4]. However, the combination of their poor processability together with the scarcity of their elements (particularly tellurium), rigidity and high cost have increased interest in searching for different types of TE materials. For this reason, conductive polymer composites (CPCs), consisting of insulating polymers modified with carbon conductive structures (i.e., carbon black, carbon nanotubes, graphene, etc.), are becoming important due to the good property balance yielded by the mechanical flexibility and low thermal conductivity of the polymer and the high electrical conductivity and Seebeck coefficient of the carbon fillers [5]. In the case of tailoring the electrical

✉ Antonio José Paleo
ajpaleovieito@2c2t.uminho.pt

1 2C2T-Centre for Textile Science and Technology, University of Minho, Guimarães, Portugal

2 Leibniz-Institut für Polymerforschung Dresden e.V. (IPF), Dresden, Germany

3 INL—International Iberian Nanotechnology Laboratory, Braga, Portugal

4 CFUM—Center of Physics of the University of Minho, Braga, Portugal

5 CICECO—Aveiro Institute of Materials, Department of Chemistry, University of Aveiro, Aveiro, Portugal

Published online: 21 June 2021

conductivity of CPCs, it is well known that non-conducting polymers display a sudden jump in σ as the content of carbon-based conductive fillers exceeds a certain critical value, known as the electrical percolation threshold ϕ_c [6]. ϕ_c determines the filler content at which a conductive network is created to allow electron or hole transport within the host polymer. Mathematically, the dependence of σ on the content of the carbon filler is written as $\sigma \propto (\phi - \phi_c)^t$ for $\phi > \phi_c$, where t is a critical exponent and ϕ is the volume fraction of the filler [7]. This simplified model predicts that below ϕ_c, the CPC has the σ value of the insulating matrix, while above ϕ_c, the σ value of the CPC approaches the σ value of the carbon filler as its content increases [8]. This means that from the intrinsic electric conductivity of the carbon fillers chosen, the highest electric conductivity of their CPCs can be estimated quite exactly from the volume fractions above ϕ_c. However, it is true that the dispersion and distribution of the carbon fillers in the polymer are also important factors that influence the final conductivity of CPCs [9]. In addition, polymer wrapping around the carbon fillers normally occurs in melt-mixing prepared CPCs [10, 11], which reduces their estimated electrical conductivity below the values of the pure carbon filler due to the contact resistance increase between adjacent particles [12]. In contrast, the highest S-values of CPCs cannot be delimited as clearly from the intrinsic S-values of the carbon fillers used. This is reflected in the paradoxical fact that, for instance, melt-mixed polypropylene (PP) composites with 2 wt. % of different commercial carbon nanotubes (CNTs) showed higher S-values than the Seebeck coefficients of the as-received multiwall carbon nanotubes (MWCNTs) Nanocyl NC 7000™, branched MWCNTs CNS-PEG, and Tuball™ single wall carbon nanotubes (SWCNTs) [13]. In this regard, decreasing S with increasing σ in CPCs is generally accepted [14, 15], which means that the Seebeck coefficient decreases while σ increases with increasing volume fraction of the carbon fillers in the polymer matrix. However, very little is known about the role of insulating polymers on the S-values of final CPCs. In this context, we have undertaken this study, which complements previous work involving the air-stable n-type TE character of melt-extruded PP composites with CNF contents varying from 0 to 5 wt. % [16]. In that precedent work, the morphological (SEM) and structural analyses (e.g., FTIR, RAMAN, and XPS) as well as the TE parameters (σ and S) at room temperature of the PP/CNF composites as a function of the wt. % of carbon nanofibers (CNFs) are discussed. In contrast, the aim of this study was to determine the real impact of polypropylene on the final TE properties of PP/CNF composites. For that purpose, the intrinsic TE values (σ and S) at 30 °C of the as-received CNFs are compared with the TE values at 30 °C of new compression-molded PP/CNF composites by using a different TE measuring system in this study. It was observed that the Seebeck coefficient values of the PP/CNF composites were always clearly less negative than the S-values of the pristine CNFs. This experimental deviation is explored by applying a semiempirical quantum chemical model that quantifies the charge carrier transfer between the outer graphitic shells of the CNFs and the surrounding polypropylene chains. This study indicates that not only the intrinsic TE properties of electrically conductive carbon fillers but also their singular charge carrier transfer with insulating polymers should be taken into account to tailor CPCs with the desired TE properties.

Experiments

Materials

A polypropylene powder, Borealis EE002AE, was used as the polymer matrix. Pyrograf®-III PR 24 LHT XT CNFs (ASI, Cedarville, OH, USA) synthesized by chemical vapor deposition (CVD) with bulk densities between 1 and 3 lb/ft^3 (0.016–0.048 g cm^{-3}) and a range of lengths of 30–100 μm were selected for producing melt-mixed polypropylene-based composites with thermoelectrical properties. Details about Pyrograf®-III CNFs can be found in previous reports [17, 18]. Briefly, this particular CNF grade is grown at 1100 °C with a thermal post-treatment of 1500 °C in an inert atmosphere, which morphologically results in a dual wall structure surrounding the hollow tubular core, as shown in Fig. 1.

Polymer composite processing

The melt-mixed PP/CNF composites were fabricated on a modular lab-scale intermeshing mini-corotating twin-screw extruder, with a screw diameter of 13 mm, a barrel length of 338 mm and an approximate L/D ratio of 26, coupled to a cylindrical rod die of ~2.85 mm diameter. A detailed description of the melt extrusion conditions has been previously published [19]. The extruded PP/CNF composites were then pelletized and compression-molded at 210 °C with a PW40HT hot press for 2 min (1.5 min preheating, max. force 50 kN, 0.5 min cooling in a minichiller, with a polyimide foil as the separation foil) into plates with a diameter of 60 mm and thickness of 0.5 mm. Thus, PP/CNF composites with different CNF concentrations from 1 to 5 wt. % were prepared.

Morphological analysis

The as-produced CNFs were imaged with a JEOL JEM-2100 electron microscope operating a LaB6 electron gun at 80 kV and acquired with an "OneView" 4k × 4k CCD

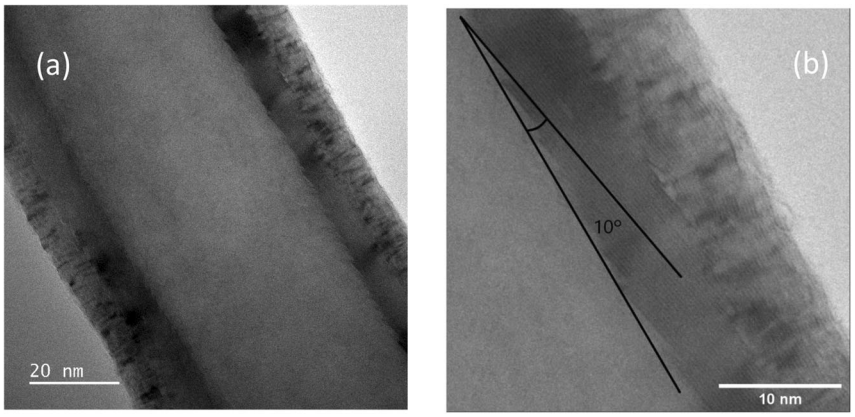

Fig. 1 **a** TEM images of carbon nanofibers PR 24 LHT XT, **b** detail of the inner layers composed of parallel graphene sheets

camera at minimal underfocus so that surface layers of the CNFs were visible. Morphological characterization of the PP/CNF composites was performed using scanning electron microscopy (SEM) by means of an Ultra plus microscope (Carl Zeiss GmbH, Germany, field emission cathode) at 3 kV. The composite strands were cryo-fractured in liquid nitrogen, and prior to observation, the surfaces were covered with 3 nm of platinum.

Electrical and thermoelectrical properties

The electric conductivity values at 30 °C of both materials (PP/CNF composites and CNF powder) were measured using a 4-wire technique. The voltage and resistance measurements were performed using a Keithley multimeter DMM2001 (Keithley Instruments, Cleveland, OH, USA). The Seebeck coefficients of the PP/CNF composites were measured from strips coated with conductive silver at their ends using a home-built TEG device at Leibniz-IPF [20, 21]. The tests were performed at 30 °C with temperature differences up to 8 K between the two copper electrodes. In the case of the CNFs, ~0.02 g of as-received CNFs in powder form were tightly filled in an open PVDF tube (inner diameter 3.8 mm, length 16 mm) without using any type of compaction pressure and then closed at each end with two T-shaped copper plugs [13]. After this, the T-shaped plugs were clamped between the copper electrodes to ensure perfect planar contact. The values of S and σ given in this study represent the mean values of eight measurements. The figure of merit of the CNF powder was estimated by using a thermal conductivity of 0.43 $W\,m^{-1}\,K^{-1}$ reported for anisotropic paper-like mats of Pyrograf®-III CNFs [22], whereas for all the PP/CNF composites, zT was estimated from the values of thermal conductivity obtained by the flash diffusivity method reported in a previous study [23]. The type of majority carriers, together with the carrier concentration n and mobility μ of PP/CNF composites, were determined by studying the Hall effect [24]. The setup, in addition to a Keithley 2410 Source Meter and 2182 Voltimeter, included a GMW 5403FG electromagnet (magnetic field up to 1 T). All Hall effect measurements were performed at room temperature for several DC current intensities using +500 mT and −500 mT on square 1.5 cm × 1.5 cm samples having a thickness of 0.5 mm with conductive silver paste coated at their corners.

Charge carrier transfer modeling

A semiempirical quantum chemical model was applied to quantify the charge carrier transfer between the outer CNF graphitic shells represented by a finite hexagonal graphene flake, as shown in Fig. 2, and the surrounding polypropylene chains. In this light, following up on a previous study [25], the molecular geometry and the charge carrier transfer of two adsorbed PP oligomers (isotactic and syndiotactic) consisting of up to 20 monomeric units and total lengths of 5 nm on a graphene flake of 5.6 nm diameter and 912 atoms was computed. The calculations were performed with the GFN1-xTB Hamiltonian, which allows computing systems with thousands of atoms [26], while the charge carrier transfer was computed by adding up the CM5 partial charges [27] of the different oligomers and the corresponding hexagonal graphene flakes.

Results and discussion

Morphological analysis

Representative TEM images of the CNFs are shown in Fig. 1. The total diameter values of 25 individual CNFs were measured and averaged, which resulted in a mean diameter of ~80 nm. This diameter is similar to the values reported by Tessonnier et al. for the same CNFs [28]. The CNFs presented a double structure, where the inner layers showed parallel graphene sheets with certain angles with respect to the hollow core. In particular, the number of inner layers in Fig. 1b was counted, which gave 22 graphene sheets with thickness values of ~0.32 nm and angles

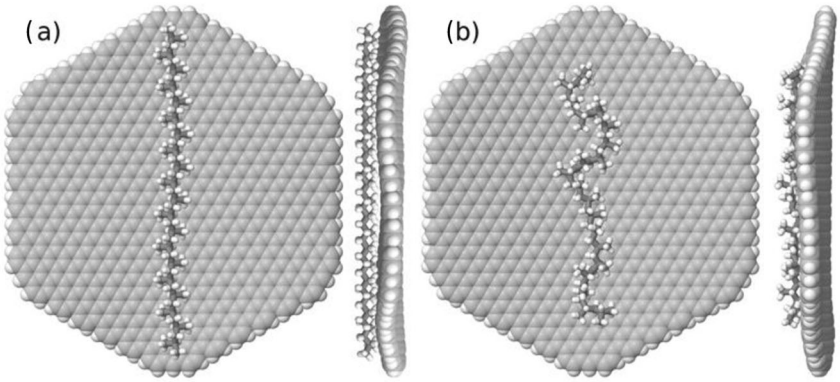

Fig. 2 Molecular geometries of (**a**) syndiotactic and (**b**) isotactic polypropylene 20-mer molecules adsorbed on a $C_{834}H_{78}$ hexagonal graphene flake computed at xTB-GFN1 level

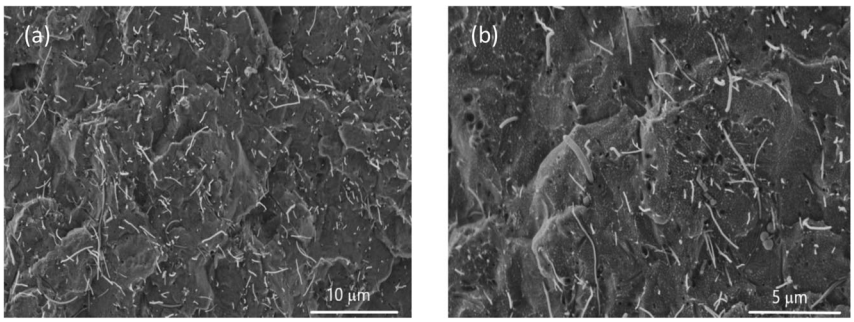

Fig. 3 SEM micrographs of PP/CNF 5 wt. % composites at low (**a**) and higher (**b**) magnifications

between them of 10°. The graphene sheets are also evident in the outer layers, although their morphology is not as regular as in the case of the inner layers. From Fig. 1b, 25 outer graphene sheets with similar dimensions of ~0.32 nm were estimated. In summary, Fig. 1a, b clearly show two different structures surrounding the hollow core. Moreover, the inner structure is clearly more ordered than the outer structure. The representative SEM micrographs of PP/CNF 5 wt. % composites are shown in Fig. 3. The CNFs protrude far above the polypropylene fracture surface, which is an indication of low wettability and poor adhesion. Despite this, the CNFs show a homogenous distribution. This can be a consequence of the post-processing debulking method used in the production of this particular CNF grade, which consists of a milling process for decreasing the diameter of the CNF agglomerates, thus making their dispersion in the PP easier [28].

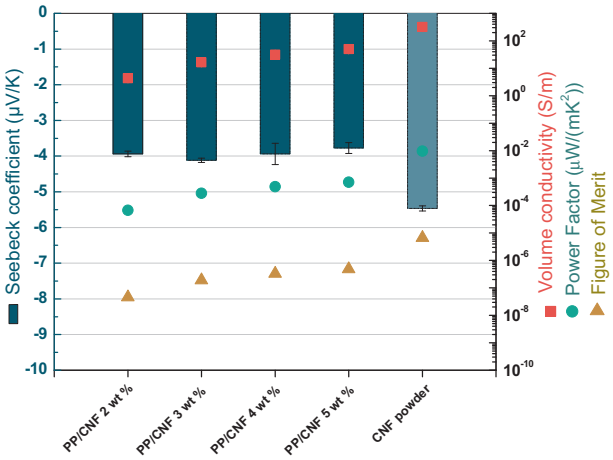

Fig. 4 Electrical conductivity (squared symbols), Seebeck coefficient (bars), power factor (circle symbols), and figure of merit (triangle symbols) of PP/CNF composites and CNF powder

Electrical and thermoelectrical analysis

The electrical conductivities of the PP/CNF composites and CNF powder at 30 °C are presented as square symbols in Fig. 4. The value of 319.8 ± 37.4 S m^{-1} (Table 1) measured for the CNF powder, equivalent to ~3×10^{-1} Ohm cm, is significantly higher than the value of 4×10^{-3} Ohm cm reported for individual Pyrograf® III CNFs [18]. These results demonstrate the great difference existing in terms of the electrical conductivity between the agglomerates, represented by the CNF powder, and the individual CNFs. That value of electrical conductivity is not significantly lower than the σ of some commercial MWCNTs, such as Nanocyl NC 7000™, where electrical conductivities of ~400 S m^{-1} were measured [13]. Interestingly, the PP/CNF composites showed conductivities from 4.3 ± 0.1 S m^{-1} in of PP/CNF 2 wt. % to 49.5 ± 0.5 S m^{-1} in of PP/CNF 5 wt. %. The increased electrical conductivity obtained as a function of the increased CNF loading is attributed to the

Table 1 Thermoelectric properties of PP-based composites filled with CNFs (electrical conductivity σ, Seebeck coefficient S, power factor PF, figure of merit zT, charge carrier concentration n, and charge carrier mobility μ)

Sample	σ (S/m)	S (μV/K)	PF (μW/mK^2)	zT	n (cm^{-3})	μ (cm^2/V s)
PP/CNF 2 wt. %	4.3 ± 0.04	−3.9 ± 0.1	$6.7 \pm 0.3 \times 10^{-5}$	4.6×10^{-8}	$1.3 \pm 0.01 \times 10^{16}$	32.2 ± 0.3
PP/CNF 3 wt. %	16.5 ± 0.2	−4.1 ± 0.1	$2.8 \pm 0.1 \times 10^{-4}$	1.9×10^{-7}	$2.0 \pm 0.1 \times 10^{17}$	11.0 ± 1.0
PP/CNF 4 wt. %	31.3 ± 0.3	−3.9 ± 0.3	$4.9 \pm 0.7 \times 10^{-4}$	3.3×10^{-7}	$8.0 \pm 1.0 \times 10^{18}$	0.24 ± 0.07
PP/CNF 5 wt. %	49.5 ± 0.5	−3.8 ± 0.2	$7.0 \pm 0.7 \times 10^{-4}$	4.8×10^{-7}	$1.3 \pm 0.4 \times 10^{19}$	0.23 ± 0.02
CNF powder	319.8 ± 37.4	−5.5 ± 0.1	$9.6 \pm 0.8 \times 10^{-3}$	6.7×10^{-6}	–	–

larger number of charge carriers injected by the CNFs, which implies higher carrier concentrations n, as confirmed by the Hall effect results (Table 1). These results match well with our previous work [16], where the electrical percolation threshold values of the PP composites melt-extruded with the same CNF grade (PR 24 LHT XT) and compression-molded under different conditions were found to be between 1 and 2 wt. %, with a critical exponent t value of 1.6, which is in agreement with the percolation theory for 3D systems [7]. Therefore, the electrical conductivity values of the PP/CNF 5 wt. % composites, which were produced with a concentration of CNFs well above ϕ_c, were lower than the electrical conductivity of the CNF powder (~320 S m^{-1}). This can be explained by the wrapping of the polypropylene chains around the CNFs, which increases the contact resistance between the adjacent CNFs, resulting in the rise of the CNF network resistivity [12]. Interestingly, the σ values of the PP/CNF 2 wt. % composites (4.3 S m^{-1}) were comparable to the σ values of melt-mixed PP/MWCNT 2 wt. % composites (3.2 S m^{-1}) presented in [13].

The bars in Fig. 4 present the Seebeck coefficients of the PP/CNF composites and CNF powder at 30 °C. The intrinsic n-type character of the CNF powder (−5.5 ± 0.1 μVK^{-1}) is very significant because it is in contrast to the results of most of the as-produced CNTs reported in the literature, which are p-type due to their oxygen doping with the environment [29]. The n-type character of the CNFs has been attributed to the fact that they can be considered nearly compensated semimetals, and their transport properties can be explained by the two-band electronic model. Thus, the partial Seebeck coefficients originating from electron and hole conduction oppose each other, resulting in small and negative S-values [30]. Another possible reason is the very low amount of oxygen (1.8%) observed by X-ray photoelectron spectroscopy (XPS) in this type of CNF [25], probably caused by the highly ordered type of the CNF external layer, which could prevent the grafting of oxygen functional groups on them and their subsequent p-doping. These results are similar to the values reported in free-standing MWCNT films grown by CVD at 800 °C [31] and the −6 μVK^{-1} reported for MWCNT buckypapers grown by CVD at temperatures above 770 °C [32]. Noticeably, the latter study explains that the negative Seebeck values of the used MWCNT buckypapers may be induced by the intrinsic n-type contribution from the inner shells, which can counteract the p-type contribution caused by the oxygen doping of the outer shells. However, the S-values found for CNFs in our study are lower than those reported for nitrogen-doped MWCNT powders [33], where negative Seebeck coefficients up to −13.8 μVK^{-1} were achieved, and they are also lower than the S-values of −38 μVK^{-1} obtained in SWCNTs encapsulated with 1,1′-bis(diphenylphosphino)-ferrocene [34]. Higher Seebeck coefficients close to −60 μVK^{-1} have been reported in SWCNTs treated with salts and crown ether [35], and even S-values of −77 μVK^{-1} have been achieved by the combination of CNT reduction with $NaBH_4$ and polyethyleneimine (PEI) wrapping [36]. In any case, the results presented here demonstrate that air-stable n-type CNFs can be directly obtained on a large scale by conventional CVD without using any of the complex methods described in those works. The PP/CNF composites also showed negative Seebeck coefficients from −3.9 ± 0.1 μVK^{-1} for PP/CNF 2 wt. % to −3.8 ± 0.2 μVK^{-1} for PP/CNF 5 wt. %. These Seebeck coefficients were lower (in absolute value) than the values of ~−8.5 μVK^{-1} measured in our preceding work by using different equipment (MMR's Seebeck System) [16]. Although CPCs generally show a decrease in S when σ increases as a consequence of the higher amount of conductive particles in the polymer [15], a constant S has also been observed in CPCs with low contents of carbon nanostructures, as observed in this study [16]. Overall, these S-values are clearly less negative than the S of the CNF powder measured (−5.5 ± 0.1 μVK^{-1}). This difference is in line with the results reported in [13], where the positive S-values of melt-mixed PP/CNT composites were higher than the corresponding S-values of the CNT powders. However, this finding will be discussed properly in the following section. Moreover, it cannot be ignored that the charge carrier mobility μ decreases significantly with increasing CNF content of the PP/CNF composites (Table 1). A similar behavior was also observed in melt-mixed PP/SWCNT composites [37] and may be due to the denser filler network created by the higher amount of CNFs present in the PP. This phenomenon could increase the number of scattering obstacles and trap sites in the charge carrier paths, effectively reducing the charge carrier mobility [38]. In comparative terms, the Seebeck coefficients of the PP/CNF composites presented here are far from the −56.6 μVK^{-1} achieved in melt-extruded PP/SWCNT composites filled with 2 wt. % of SWCNTs and 5 wt. % of

copper oxide (CuO) [37]. However, the authors had to add 8 wt. % polyethylene glycol (PEG) during extrusion to obtain n-type CPCs.

The PFs at 30 °C of the PP/CNF composites and CNF powder were calculated, and the results are shown as circle symbols in Fig. 4. The CNF powder shows the highest PF of $9.6 \times 10^{-3} \pm 0.8 \times 10^{-3}$ μW/mK^2, whereas the PP/CNF 5 wt. % composites achieved a PF of $7.0 \times 10^{-4} \pm 0.7 \times 10^{-4}$ μW/mK^2 (lower than the PF of 1.75×10^{-3} obtained in our previous work in PP/CNF 5 wt. % composites [16]). A comparison with the literature shows that the PF of PP/CNF 2 wt. % (6.7×10^{-5} μW/mK^2) is lower than those of some melt-mixed PP composites with 2 wt. % of NC 7000^{TM} MWCNTs (1.0×10^{-4} μW/mK^2), MWCNT CNS-PEG (2.9×10^{-2} μW/mK^2) or Tuball^{TM} SWCNTs (2.7×10^{-2} μW/mK^2) [13]. In this respect, it should be noted that values as high as 0.11 μW/mK^2 have been recently reported in melt-mixed PP composites with 2 wt. % of p-type boron-doped SWCNTs [39].

The estimated zT of the CNF powder, shown as triangle symbols in Fig. 4, presented a value of 6.7×10^{-6}, which is on the order of magnitude of that of MWCNT buckypapers grown by CVD at temperatures above 770 °C [15] but far from the zT of 10^{-1} reported for SWCNTs treated with salts and crown ether [35]. Likewise, the highest zT of 4.8×10^{-7} for PP/CNF 5 wt. % composites (lower than the value of 1.2×10^{-6} of our preceding work [16] for PP/CNF 5 wt. % composites) was calculated by using a thermal conductivity of 0.44 W m^{-1} K^{-1} measured in [23], and the values of σ and S presented in this study. This value of zT was lower than the values of 1.3×10^{-4} and 3.3×10^{-5} of PP composites melt-mixed with 2 wt. % of boron-doped SWCNTs [39] and 2 wt. % of MWCNT CNS-PEG [13], respectively.

Electron donation from the outer layers of the CNFs to the polypropylene

As noted above, the Seebeck coefficient of the CNF powder (−5.5 μVK^{-1}) was different from the S measured in PP/CNF 5 wt. % composites (−3.8 μVK^{-1}). This finding led to the hypothesis that the polypropylene host could have an active role in the intensity of the S-values obtained in the PP/CNF composites despite its insulating character. To better understand this hypothesis, the effect of absorbed syndiotactic/isotactic PP chains on most external graphene CNF flakes was modeled as described in the previous charge carrier transfer modeling section. The model yields binding energies on hexagonal graphene flakes of 0.20 and 0.19 eV/monomer for two syndiotactic and isotactic 20-mers, respectively. The model also shows that tacticity and conformation freedom should not play a determinant role. Interestingly, a small but reproducible charge carrier transfer from the graphene to the PP molecules, exactly 2×10^{-3} electrons per monomer, was found for both types of tacticity. According to this, the CNF outer layers are predicted to have a very slight electron donation towards the surrounding PP molecular chains, which could explain the lower value of S (absolute value) found in the PP/CNF 5 wt. % composites. From this analysis, we may expect the same electron donation of other similar carbon structures, such as CNTs, to the surrounding PP in common p-type PP/CNT composites [13, 39], which would imply an increase in the p-type character of the pristine CNTs and consequently an increase in the intensity of their positive Seebeck coefficients. Specifically, this has been observed in melt-mixed composites consisting of polypropylene (Moplen HP400R) and different types of CNTs [13]. Therefore, this hypothesis could explain the higher Seebeck coefficients observed in PP/CNT composites with 2 wt. % of Nanocyl NC 7000 ^{TM} MWCNTs (9.5 μVK^{-1}), branched CNS-PEG MWCNTs (17.5 μVK^{-1}), and Tuball^{TM} SWCNTs (47.2 μVK^{-1}), with respect to the S-values of their corresponding CNT powders: 6.3 μVK^{-1} (Nanocyl NC 7000 ^{TM}), 10.1 μVK^{-1} (branched MWCNTs CNS-PEG), and 39.6 μVK^{-1} (SWCNT Tuball^{TM}).

Conclusions

The TE properties of commercial vapor-grown CNFs produced by CVD with graphitic tubular cores surrounded by two different layers and their melt-extruded polypropylene composites were compared. The as-received CNFs present an electrical conductivity of ~320 S m^{-1} and an interesting phenomenon of showing negative S-values of −5.5 μVK^{-1}. In contrast, the PP/CNF composites with 5 wt. % of CNFs showed a conductivity of ~50 S m^{-1} and a negative Seebeck coefficient of −3.8 μVK^{-1}. Therefore, the S of the PP/CNF 5 wt. % composites is less negative than the Seebeck coefficient of the as-received CNFs. This change can be attributed to a small but yet quantifiable electron-donating effect arising from the most external graphene layers of the CNFs to the PP molecules, as revealed by a semiempirical quantum chemical model, which could slightly reduce the n-type character of the pristine CNFs. Our study indicates that even insulating polymers such as PP may have a quantifiable effect on the intrinsic Seebeck coefficient of carbon-based nanostructures, and this fact should also be taken into consideration to tailor CPCs with the desired TE properties.

Acknowledgements The authors affiliated with 2C2T acknowledge support from FCT-Foundation for Science and Technology within the scope of project UID/CTM/00264/2020. The authors would like to thank the staff of the IPF's Research Technology Department for their support with the TE measuring device, and they appreciate the help of Mrs. Manuela Heber in the SEM study and Dr. Oliver Schraidt from INL in the TEM analysis. In addition, support through project IF/

00894/2015 and within the scope of the project CICECO-Aveiro Institute of Materials, UIDB/50011/2020 and UIDP/50011/2020 and access to the Navigator platform (LCA-UC) through the Advanced Computing Project CPCA/A2/2524/2020, financed by national funds through the Portuguese Foundation for Science and Technology I.P./MCTES, is gratefully acknowledged.

Compliance with ethical standards

Conflict of interest The authors declare no competing interests.

Publisher's note Springer Nature remains neutral with regard to jurisdictional claims in published maps and institutional affiliations.

References

1. Gayner C, Kar KK. Recent advances in thermoelectric materials. Prog Mater Sci. 2016;83:330–82. https://doi.org/10.1016/j.pmatsci.2016.07.002.
2. Rowe DM. CRC handbook of thermoelectrics. Boca Raton, FL: CRC press; 1995.
3. Blackburn JL, Ferguson AJ, Cho C, Grunlan JC. Carbon-nanotube-based thermoelectric materials and devices. Adv Mater. 2018;30. https://doi.org/10.1002/adma.201704386.
4. Tan G, Zhao LD, Kanatzidis MG. Rationally designing high-performance bulk thermoelectric materials. Chem Rev. 2016;116:12123–49. https://doi.org/10.1021/acs.chemrev.6b00255.
5. McGrail BT, Sehirlioglu A, Pentzer E. Polymer composites for thermoelectric applications. Angew Chem Int Ed. 2015;54:1710–23. https://doi.org/10.1002/anie.201408431.
6. Nigro B, Grimaldi C, Ryser P. Tunneling and percolation transport regimes in segregated composites. Phys Rev E. 2012;85. https://doi.org/10.1103/PhysRevE.85.011137.
7. Stauffer D, Aharony A. Introduction to percolation theory. London: Taylor & Francis; 1992.
8. McLachlan DS, Chiteme C, Park C, Wise KE, Lowther SE, Lillehei PT, Siochi EJ, Harrison JS. AC and DC percolative conductivity of single wall carbon nanotube polymer composites. J Polym Sci Part B Polym Phys. 2005;43:3273–87. https://doi.org/10.1002/polb.20597.
9. Alig I, Pötschke P, Lellinger D, Skipa T, Pegel S, Kasaliwal GR, Villmow T. Establishment, morphology and properties of carbon nanotube networks in polymer melts. Polymer. 2012;53:4–28. https://doi.org/10.1016/j.polymer.2011.10.063.
10. Chen J, Liu B, Gao X, Xu D. A review of the interfacial characteristics of polymer nanocomposites containing carbon nanotubes. RSC Adv. 2018;8:28048–85. https://doi.org/10.1039/c8ra04205e.
11. Baudouin AC, Devaux J, Bailly C. Localization of carbon nanotubes at the interface in blends of polyamide and ethylene-acrylate copolymer. Polymer. 2010;51:1341–54. https://doi.org/10.1016/j.polymer.2010.01.050.
12. Li C, Thostenson ET, Chou TW. Dominant role of tunneling resistance in the electrical conductivity of carbon nanotube-based composites. Appl Phys Lett. 2007;91. https://doi.org/10.1063/1.2819690.
13. Krause B, Barbier C, Levente J, Klaus M, Pötschke P. Screening of different carbon nanotubes in melt-mixed polymer composites with different polymer matrices for their thermoelectrical properties. J Compos Sci. 2019;3:106.
14. Kaiser AB. Thermoelectric power and conductivity of heterogeneous conducting polymers. Phys Rev B. 1989;40:2806–13. https://doi.org/10.1103/PhysRevB.40.2806.
15. Hewitt CA, Kaiser AB, Roth S, Craps M, Czerw R, Carroll DL. Varying the concentration of single walled carbon nanotubes in thin film polymer composites, and its effect on thermoelectric power. Appl Phys Lett. 2011;98. https://doi.org/10.1063/1.3580761.
16. Paleo AJ, Vieira EMF, Wan K, Bondarchuk O, Cerqueira MF, Goncalves LM, Bilotti E, Alpuim P, Rocha AM. Negative thermoelectric power of melt mixed vapor grown carbon nanofiber polypropylene composites. Carbon. 2019;150:408–16. https://doi.org/10.1016/j.carbon.2019.05.035.
17. Tibbetts GG, Lake ML, Strong KL, Rice BP. A review of the fabrication and properties of vapor-grown carbon nanofiber/polymer composites. Compos Sci Technol. 2007;67:1709–18. https://doi.org/10.1016/j.compscitech.2006.06.015.
18. Al-Saleh MH, Sundararaj U. A review of vapor grown carbon nanofiber/polymer conductive composites. Carbon. 2009;47:2–22. https://doi.org/10.1016/j.carbon.2008.09.039.
19. Paleo AJ, Sencadas V, Van Hattum FWJ, Lanceros-Méndez S, Ares A. Carbon nanofiber type and content dependence of the physical properties of carbon nanofiber reinforced polypropylene composites. Polym Eng Sci. 2014;54:117–28. https://doi.org/10.1002/pen.23539.
20. Jenschke W, Ullrich M, Krause B, Pötschke P. Messanlage zur Untersuchung des Seebeck-Effektes in polymermaterialien measuring apparatus for study of Seebeck effect in polymer materials. Technisches Mess. 2020;87:495–503. https://doi.org/10.1515/teme-2019-0152.
21. Gnanaseelan M, Chen Y, Luo J, Krause B, Pionteck J, Pötschke P, Qi H. Cellulose-carbon nanotube composite aerogels as novel thermoelectric materials. Compos Sci Technol. 2018;163:133–40. https://doi.org/10.1016/j.compscitech.2018.04.026.
22. Mahanta NK, Abramson AR, Lake ML, Burton DJ, Chang JC, Mayer HK, Ravine JL. Thermal conductivity of carbon nanofiber mats. Carbon. 2010;48:4457–65. https://doi.org/10.1016/j.carbon.2010.08.005.
23. Paleo AJ, García X, Arboleda-Clemente L, Van Hattum FW, Abad MJ, Ares A. Enhanced thermal conductivity of rheologically percolated carbon nanofiber reinforced polypropylene composites. Polym Adv Technol. 2015;26:369–75. https://doi.org/10.1002/pat.3462.
24. ASTM F76-08 (2016)e1 Standard test methods for measuring resistivity and hall coefficient and determining hall mobility in single-crystal semiconductors.
25. Paleo AJ, Vieira EMF, Wan K, Bondarchuk O, Cerqueira MF, Bilotti E, Melle-Franco M, Rocha AM. Vapor grown carbon nanofiber based cotton fabrics with negative thermoelectric power. Cellulose. 2020;27:9091–104. https://doi.org/10.1007/s10570-020-03391-4.
26. Grimme S, Bannwarth C, Shushkov P:. A robust and accurate tight-binding quantum chemical method for structures, vibrational frequencies, and noncovalent interactions of large molecular systems parametrized for all spd-block elements (Z = 1-86). J Chem Theory Comput. 2017;13:1989–2009. https://doi.org/10.1021/acs.jctc.7b00118.
27. Marenich AV, Jerome SV, Cramer CJ, Truhlar DG. Charge model 5: An extension of hirshfeld population analysis for the accurate description of molecular interactions in gaseous and condensed phases. J Chem Theory Comput. 2012;8:527–41. https://doi.org/10.1021/ct200866d.
28. Tessonnier JP, Rosenthal D, Hansen TW, Hess C, Schuster ME, Blume R, Girgsdies F, Pfänder N, Timpe O, Su DS, Schlögl R. Analysis of the structure and chemical properties of some commercial carbon nanostructures. Carbon. 2009;47:1779–98. https://doi.org/10.1016/j.carbon.2009.02.032.
29. Zettl A. Extreme oxygen sensitivity of electronic properties of carbon nanotubes. Science. 2000;287:1801–4. https://doi.org/10.1126/science.287.5459.1801.

30. Stokes KL, Tritt TM, Fuller-Mora WW, Ehrlich AC, Jacobsen RL. Electronic transport properties of highly conducting vapor-grown carbon fiber composites. In: International Conference on Thermoelectrics, Pasadena, CA, USA, ICT, Proceedings; 1996. pp. 164–7.
31. Kumanek B, Stando G, Wróbel PS, Janas D. Impact of synthesis parameters of multi-walled carbon nanotubes on their thermoelectric properties. Materials. 2019;12:1–13. https://doi.org/10.3390/ma12213567.
32. Hewitt CA, Kaiser AB, Craps M, Czerw R, Carroll DL. Negative thermoelectric power from large diameter multiwalled carbon nanotubes grown at high chemical vapor deposition temperatures. J Appl Phys. 2013;114. https://doi.org/10.1063/1.4819104.
33. Krause B, Konidakis I, Arjmand M, Sundararaj U, Fuge R, Liebscher M, Hampel S, Klaus M, Serpetzoglou E, Stratakis E, Pötschke P. Nitrogen-doped carbon nanotube/polypropylene composites with negative seebeck coefficient. J Compos Sci. 2020;4:14.
34. Nonoguchi Y, Iihara Y, Ohashi K, Murayama T, Kawai T. Air-tolerant fabrication and enhanced thermoelectric performance of n-type single-walled carbon nanotubes encapsulating 1,1′-Bis (diphenylphosphino)ferrocene. Chem Asian J. 2016;11:2423–7. https://doi.org/10.1002/asia.201600810.
35. Nonoguchi Y, Nakano M, Murayama T, Hagino H, Hama S, Miyazaki K, Matsubara R, Nakamura M, Kawai T. Simple salt-coordinated n-type nanocarbon materials stable in air. Adv Funct Mater. 2016;26:3021–8. https://doi.org/10.1002/adfm.201600179.
36. Yu C, Murali A, Choi K, Ryu Y. Air-stable fabric thermoelectric modules made of N- and P-type carbon nanotubes. Energy Environ Sci. 2012;5:9481–6. https://doi.org/10.1039/c2ee22838f.
37. Luo J, Cerretti G, Krause B, Zhang L, Otto T, Jenschke W, Ullrich M, Tremel W, Voit B, Pötschke P. Polypropylene-based melt mixed composites with singlewalled carbon nanotubes for thermoelectric applications: Switching from p-type to n-type by the addition of polyethylene glycol. Polymer. 2017;108:513–20. https://doi.org/10.1016/j.polymer.2016.12.019.
38. Smith RC, Liang C, Landry M, Nelson JK, Schadler LS. The mechanisms leading to the useful electrical properties of polymer nanodielectrics. IEEE Trans Dielectr Electr Insulation. 2008;15:187–96. https://doi.org/10.1109/T-DEI.2008.4446750.
39. Krause B, Bezugly V, Khavrus V, Ye L, Cuniberti G, Pötschke P. Boron doping of SWCNTs as a way to enhance the thermoelectric properties of melt-mixed polypropylene/SWCNT composites. Energies. 2020;13. https://doi.org/10.3390/en13020394.